

PACS numbers: 42.65.Dr; 42.65.Es; 42.65.Tg; 42.65.Ky
DOI: 10.1070/QE2012v042n12ABEH015003

Properties of dark solitons under SBS in focused beams

I.M. Bel'dyugin, A.I. Erokhin, V.F. Efimkov, I.G. Zubarev, S.I. Mikhailov

Abstract. **Using the method of four-wave probing of the waist of the laser beam focused into the bulk of a short active medium ($L << \tau c$, where L is the length of the active medium, τ is the pulse duration, and c is the speed of light), we have studied the dynamics of the behaviour of a dark soliton, appearing upon a jump of the input Stokes signal phase by about π under SBS. The computer simulation has shown that when spontaneous noises with the gain increment Γ, exceeding the self-reflection threshold by 2 – 3 times, are generated, the dark soliton propagates along the interaction region for the time $t \approx T_2\Gamma_{th}/2$, where T_2 is the the lifetime of acoustic phonons, and Γ_{th} = 25 – 30 is the stationary threshold gain increment.**

Keywords: *SBS, dark solitons, four-wave mixing.*

1. Introduction

Numerous experimental works devoted to the study of SBS and to application of the phase conjugation effect employ a widespread scheme of tight focusing of pump radiation into the bulk of the active medium [1, 2] (note that researchers had used the scheme before the discovery of the phase conjugation effect [3]). However, even in the regime of strong saturation, strong fluctuations of the output Stokes signal amplitude may arise [4, 5], which are associated with the fast changes by about π of the phase of the noise Stokes field at the time of its 'fading' (see, e.g., [6]).

As will be shown in this paper, as a result of a sequential erasing and recording of acoustic grating vibrations, solitary waves with amplitude – phase modulation can be generated. By analogy with the known Raman solitons [7, 8], they can be called Brillouin solitons. A detailed discussion of Raman solitons can be found in paper [8], which contains an extensive list of publications. A characteristic manifestation of Brillouin solitons is strong amplitude modulation of the output Stokes signal, which is observed as a decrease in intensity followed by a sharp increase and attainment of the stationary regime. As an example, Fig. 1 shows the oscillogram of the output Stokes signal recorded due to SBS from spontaneous noises in titanium tetrachloride by focusing a single-mode single-frequency pump pulse at a wavelength λ = 1.055 μm into the bulk of the active medium. It should be noted that the appearance or absence of such modulation is of statistical character. It is this circumstance that may significantly affect the stability of the time parameters of phase-conjugate mirrors and SBS combiners [9]. The purpose of this paper is to study experimentally the formation of a soliton-like structure under SBS, i.e., when the interacting waves counterpropagate, to determine the velocity of its motion, and to describe theoretically the results obtained. To determine the time parameters of this process, we have developed an experimental technique based on the use of the probe radiation, constructed a mathematical model of the experiment, carried out the experiments and compared their results with the results of calculations by the computer model.

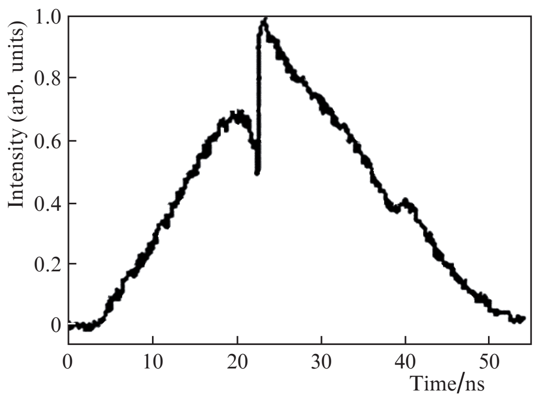

Figure 1. Oscillogram of the Stokes pulse with a characteristic intensity jump.

2. Study of the soliton regime of operation of the weak-signal SBS amplifier

The main idea of the probe pulse is based on the results of paper [10], which studied theoretically and experimentally the mechanism of transient four-wave mixing in the Brillouin nonlinearity to obtain weak signals under phase conjugation conditions. Figure 2 shows a simplified scheme of the setup for the relevant experiments. Radiation (*1*) of a single-mode single-frequency passively Q-switched neodymium phosphate glass laser emitting a beam of diameter ~3 mm was focused through a plane-parallel plate (*2*) by a lens (*4*) with a focal length of 20 cm in the centre of the cell (*5*) with an active medium (e.g. carbon tetrachloride or titanium tetrachloride).

A.I. Erokhin, V.F. Efimkov, I.G. Zubarev, S.I. Mikhailov P.N. Lebedev Physics Institute, Russian Academy of Sciences, Leninsky prosp. 53, 119991 Moscow, Russia; e-mail: aerokhin@sci.lebedev.ru, efimkov@sci.lebedev.ru, zubarev@sci.lebedev.ru, smekaelov@mailfrom.ru

Received 16 July 2012; revision recieved 24 September 2012
Kvantovaya Elektronika **42** (12) 1087 – 1092 (2012)
Translated by I.A. Ulitkin

This radiation was used as a pump to obtain SBS from spontaneous noises. In similar conditions, the phase-conjugation regime is realised and a Stokes signal reflected from the cell has the wave front with the phase coupled with the phase front of the pump, i.e., propagates backwards. In addition, the pump radiation, twice reflected from the inner surfaces of the plate, formed a weak probe beam that was parallel to the pump beam. Then, the probe beam was also focused in the centre of the cell, where it intersected with the pump beam.

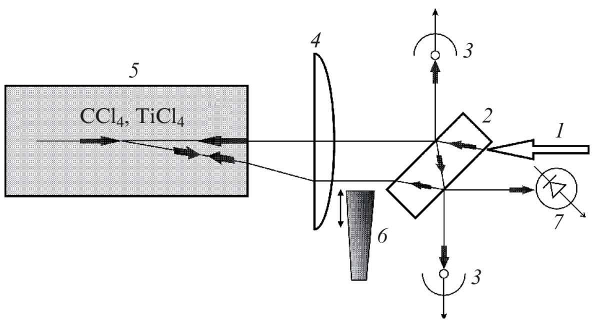

Figure 2. Setup of the experiment (see notations in the text).

As a result, in addition to the pump radiation reflected backwards, there emerges a Stokes signal propagating toward the probe beam. By placing a glass wedge (*6*) in the beam, we can change the point of intersection of the beams without going out of the focal region. Photodetectors (*3*) and (*7*) were used for recording the time dependence of the powers of the pump wave, reflected Stokes pulse and reflected Stokes pulse of probe radiation. At the same time, the temporal shapes of the laser pulse and the SBS signal were recorded with a FK-19 photodetector (*3*), and the temporal shape of the signal resulting from the four-wave mixing and having a much lower intensity was recorded with a Hamamatsu S5973 pin-diode (*7*). The signals from the photodetectors were fed to a multi-channel high-speed Tektronix TDS 3032 oscilloscope. The time resolution of the registration system was ~1 ns.

We also carried out computer simulations of the experiment. An important point in the formulation of such experiments should be mentioned, i.e., synchronisation of two recording channels: main Stokes pulse and probe Stokes pulse. In our case we used a simple trick: in the scheme in Fig. 2, instead of the cell with the active medium, we placed in the focal plane of the focusing lens a flat mirror located perpendicular to the bisector of the angle of convergence of the main and reference beams. The beams reflected from the mirror served as reference ones for adjusting the registration system.

2.1. Main results of the experiment

As mentioned above, the pump pulse was a single-mode and single frequency pulse. The FWHM pulse duration ranged from 40 to 100 ns by changing the length of the resonator of the master oscillator and by employing passive switches with different optical density, based on LiF crystals with F-colour centres. Figure 3 shows a typical oscillogram of the pump pulse. Note that the shape of the pump pulse is well approximated by a Gaussian function, which was used in the computer simulation. The transverse beam size was ~3 mm at an angle of divergence of $\theta \sim 4 \times 10^{-4}$ rad. The energy of the pump pulse was varied by means of filters and exceeded the threshold of the SBS appearance by two or three times. The length of the cell with the active medium was 40 cm. The characteristic lifetime of acoustic phonons was $T_2 = 0.6$ and 1.5 ns for CCl_4 and $TiCl_4$, respectively.

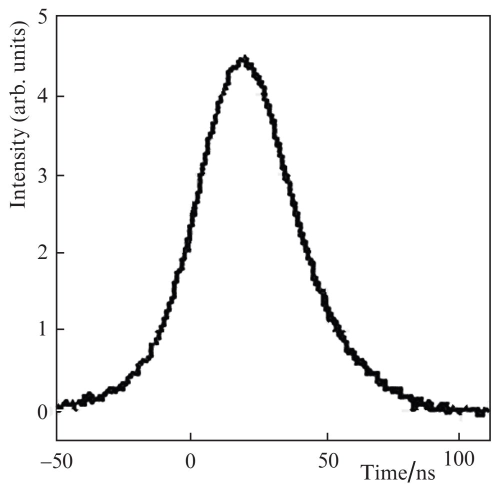

Figure 3. Oscillogram of the pump pulse.

Figure 4 shows the pulse oscillograms of the output Stokes signal and the signal arrived from the probe channel. We note again that a sampling of the results was obtained using ~1000 pump pulses. It is clearly seen that the minima of the spikes of the Stokes signal at the output lag behind the corresponding minima in the probe channel. Averaging the experimental data from a sample of about 50 pulses for each active medium yielded an average time delay of 3.5 ± 1 ns for CCl_4 and 8.5 ± 1 ns for $TiCl_4$. Knowing the time delay, we can estimate the velocity of propagation of the minima of the Stokes signal, which will be done later. Note also complete time similarity (up to a ratio of the lifetimes of acoustic phonons) of the oscillograms shown in Fig. 4. Shifting the probed region with a glass wedge (*6*) (see Fig. 2) by about 3 mm in the direction of the entrance window of the cell, we significantly reduced the time delay. This is obviously due to the fact that for a Gaussian beam half of the gain increment occurs in the region of its caustic. Moving the region of four-wave interaction in the opposite direction weakens four-wave mixing, such that we failed to reliably distinguish the signal on the photodiode (*7*) from the noise.

2.2. Theoretical analysis, construction of a computer model and discussion of the results

Let us perform the analysis, assuming that the active medium is short ($L \ll \tau c$, where L is the length of the active medium, τ is the duration of interacting light pulses, and c is the speed of light), which corresponds to the experimental situation (here we do not consider variants associated with the Stokes pulse compression because of the group delay effects). Then, time derivatives can be ignored in the equations for the light fields. Here, we believe that the interaction has a character that is local with respect to the response of the active medium and neglect the spatial derivatives, which is valid for the small lifetime of the acoustic oscillations T_2 and also in line with the experimental situation. The final system of dynamic equa-

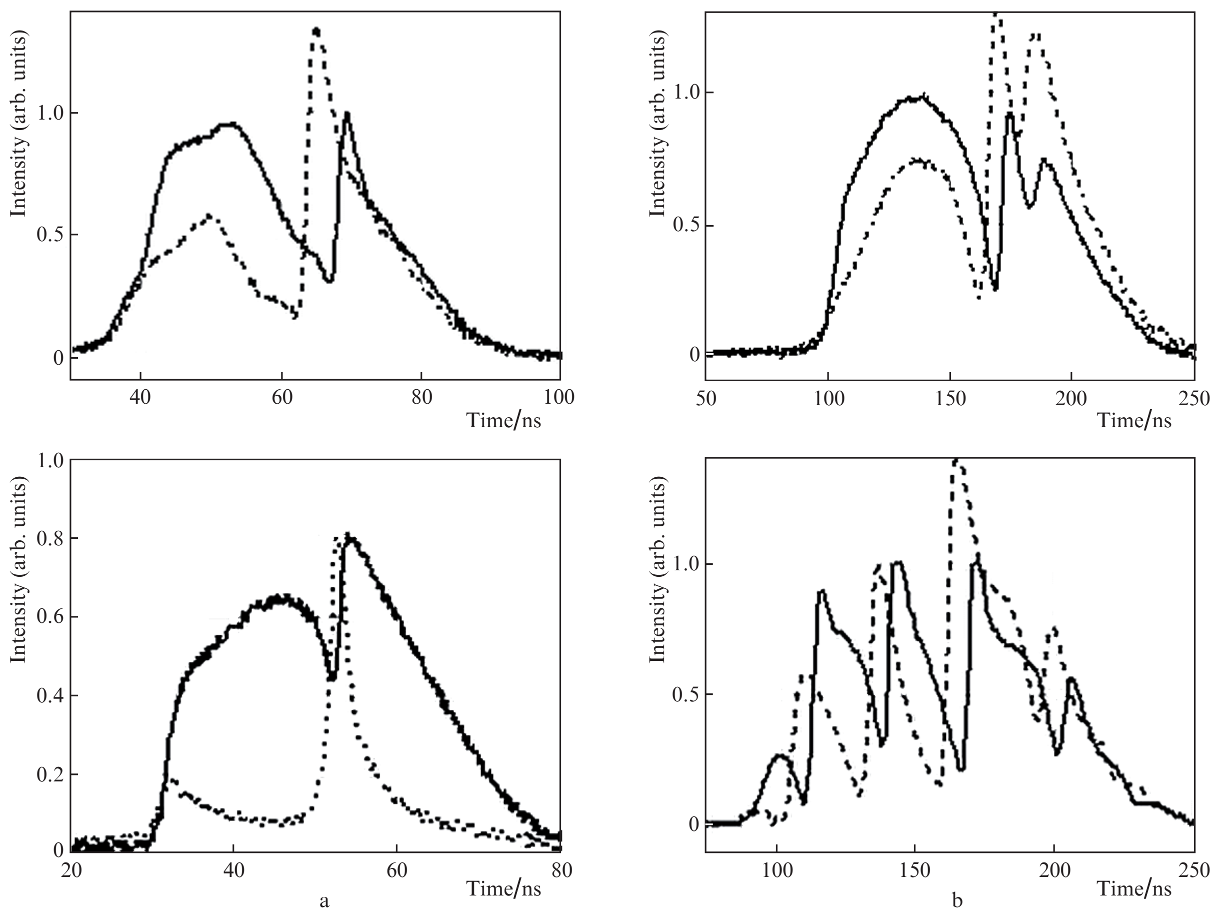

Figure 4. Two implementations of the pulse oscillograms of the output Stokes radiation (solid curves) and the radiation reflected in the probe channel (dashed curves) for CCl_4 (a) and $TiCl_4$ (b).

tions for counterpropagating plane waves, in accordance with the scheme of interaction (see Fig. 2), has the form:

$$\frac{\partial a(z,t)}{\partial z} = 0.5g_0 A(z,t)q^*(z,t),$$

$$\frac{\partial A(z,t)}{\partial z} = 0.5g_0 a(z,t)q(z,t), \qquad (1)$$

$$T_2\frac{\partial q(z,t)}{\partial t} + q(z,t) = A(z,t)a^*(z,t) + F(z,t).$$

Here z is the longitudinal coordinate of propagation; g_0 is the SBS gain; $A(z,t)$ is a slowly varying amplitude of the pump wave; $a(z,t)$ is a slowly varying amplitude of the counterpropagating weak wave; $q(z,t)$ is a slowly varying amplitude of acoustic waves; and $F(z,t)$ is a delta-correlated random force, caused by density fluctuations.

System (1) was solved numerically using the boundary and initial conditions with $F(z,t)$ being modelled with the help of two known Rnd functions: $F(z,t) = R\mathrm{Rnd}(1) \times \exp[\mathrm{iRnd}(2\pi)]$ at each point of the difference scheme. Its amplitude R was chosen such that in the absence of an input Stokes signal, in a stationary regime the Stokes intensity of the output signal for the scattering gain increment $\sim$30 was $\sim$0.01 of the pump intensity, which is usually the experimental threshold of SBS detection. The numerical solution of system (1) represented a space–time matrix of amplitudes of the pump wave, the counterpropagating and acoustic waves, which allowed one to obtain the basic characteristics (phase and intensity) in any arbitrary space–time section. This is the main difference of our approach to this problem from the approach of a number of authors [11, 12], who in their calculations were only interested in the output characteristics of the Stokes signal and output pump wave. What we are primarily interested in is how the process occurs in the active medium. The temporal shape of the pump pulses was selected on the basis of our experimental data.

First, we modelled the amplification of the external Stokes signal for a phase jump by π and the signal attenuation with respect to the input pump by 10^{13} times. Such attenuation corresponds to the experimental threshold of the SBS appearance in the stationary regime. The Stokes signal intensity distribution along the interaction length at different points in time is shown in Fig. 5. It is clearly seen that when the input signal phase jumps by π, an ‘attenuation wave’ is formed and the Stokes signal is amplified in the active medium. This is explained by the mechanism of successive ‘erasure’ of the acoustic wave with the old phase and recording of a wave with a new phase. In the case of generation from spontaneous noises, the appearance of such pulses is stochastic in nature, which is manifested in the observed strong changes in the temporal shape of the output Stokes signal from one laser shot to another (see Fig. 4).

Figure 6 presents similar distributions for the case of the generation from spontaneous noises. The velocity of propagation of the Stokes signal minimum corresponded to the

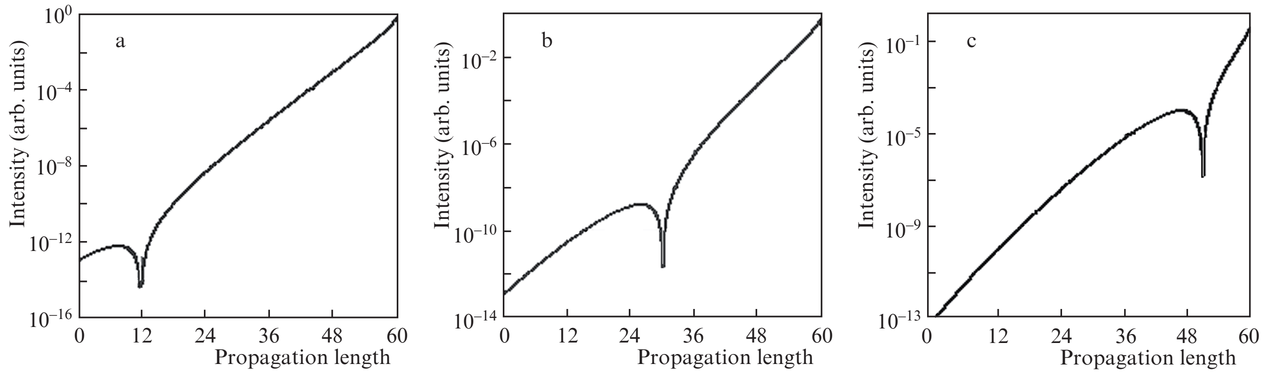

Figure 5. Stokes signal intensity distribution along the propagation length z, normalised to the stationary gain increment at time $t < T_2$ (a), $t = T_2$ (b) and $t > T_2$ (c) (the time interval between adjacent frames is 2.6 ns, $T_2 = 0.6$ ns) after the phase jump by π in the regime of amplification of the external signal.

group velocity $V_g \approx L/(0.5\Gamma_{th}T_2)$, where $\Gamma_{th} \approx 25-30$ is a stationary threshold gain increment [13]. Such a behaviour of the Stokes radiation directly indicates the soliton nature of the process and corresponds to the generation of a dark soliton. The only difference is that because of the counterpropagation of interacting waves, in our case there is a tight feedback with pumping through which the approach of the minimum of the soliton intensity to the exit from the active medium is accompanied by a jump-like increase in the intensity of the pump behind the soliton. This leads to a sharp increase in the gain and, consequently, to the formation of the characteristic S-shaped signal (see Figs 1 and 4, as well as, for example, paper [4]). In the case of large excesses of the pump intensity over the observation threshold the amplitude of spikes decreases, since in the absence of group delay the instantaneous intensity of the Stokes radiation is obviously less than the instantaneous intensity of the pump. The account for the group delay effects can in our opinion lead to the stabilisation of the temporal structure of Brillouin solitons, as indicated by the results of [11, 12].

To construct a mathematical model of the above-described experiments with the probe pulse, system (1) should be supplemented by two more equations:

$$T_2\frac{\partial Q(t,z)}{\partial t} + Q(t,z) = kA(t,L)a^*\Big(t,\frac{L}{2}\Big),$$
$$\frac{\partial a_z(t,z)}{\partial z} = 0.5A\Big(t,\frac{L}{2}\Big)Q^*(t,z), \qquad (2)$$

which correspond to the four-wave mixing process on the Brillouin nonlinearity in the middle of the active region (at $z = L/2$). In (2) $Q(t,z)$ is the acoustic wave resulting from the interaction of the probe pump and main Stokes radiation and $a_z(t,z)$ is the Stokes signal in the probe channel. We believe that the interaction length of the probe beam with the main beam is sufficiently small and the main interaction occurs in the constant fields of the pump, probe pulse and main Stokes signal, which is fully consistent with experiment. Stokes signal amplification a_z in the probe pulse field in the interval $L/2 \div L$ can be neglected, because the probe pulse was obtained due to two reflections from a plane-parallel plate (Fig. 2), and its intensity is 625 times less than that of the pump, i.e., $k = 1/25$. We also neglect the gain in the pump field due to the short length of interaction. In principle, both these factors can be taken into account in the numerical solution; however, it will not lead to substantially different results, but only will increase the computation time. Joint numerical solution of (1) and (2) was in fact a virtual experiment. Obviously, if the time is given in units of T_2, the difference between the various active media will be found only in the change of time scales of the process under study, which was obtained experimentally (see Section 2.1).

Figure 7 presents the pulse shapes of the Stokes signal and the signal reflected toward the probe radiation, obtained as a result of the virtual experiment. A comparison of these data with the results of the experiment (Fig. 4) shows that the numerical experiment adequately describes the real experi-

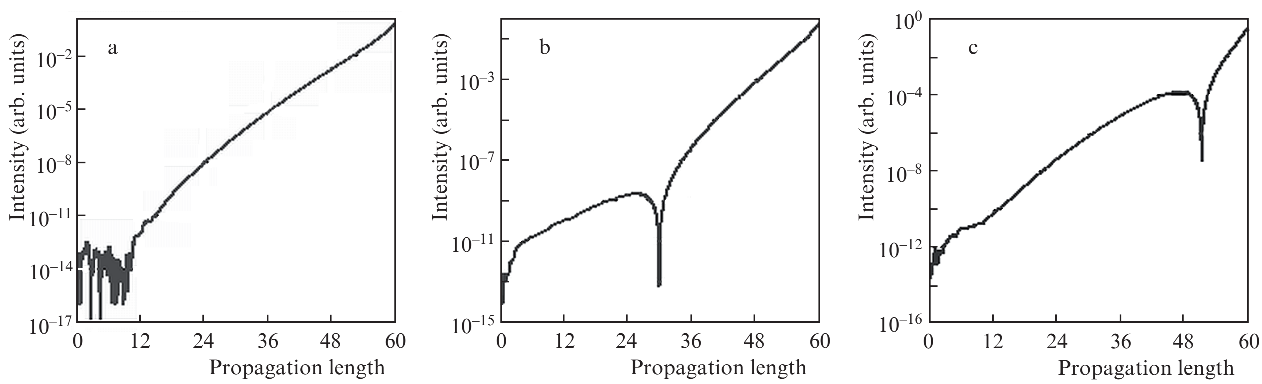

Figure 6. Same as in Fig. 5, but for SBS from spontaneous noises.

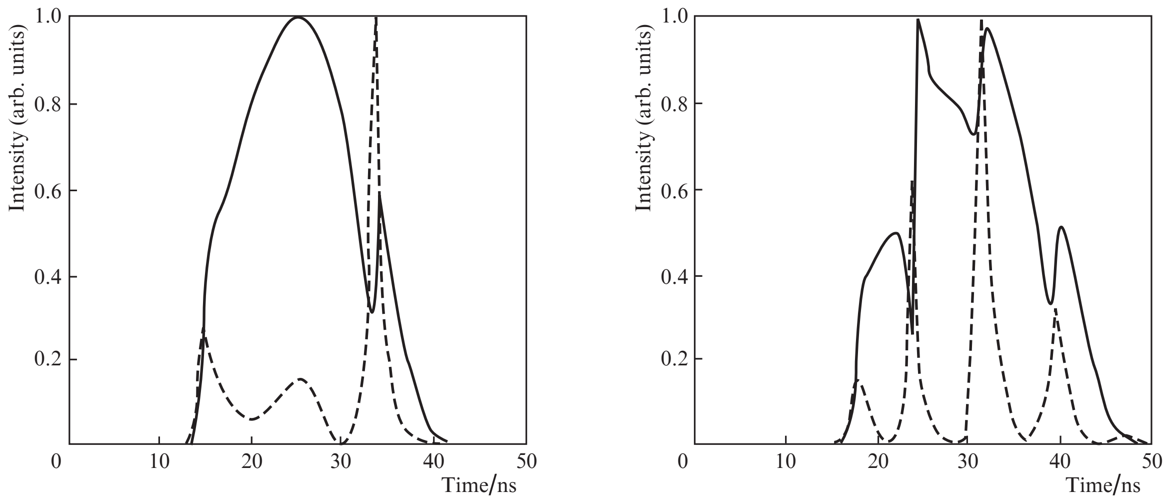

Figure 7. Results of computer simulation of the experiment: solid curves represent the output Stokes signal, dashed curves – the signal in the probe channel (taken into account are the delay of the signal for the time $\sim T_2$ relative to the main Stokes signal).

mental situation and can serve as a basis for the selection of the Brillouin active media, as well as for optimisation of a number of parameters of the SBS combiners. Figure 8 shows the calculated time dependences of the intensity and phase of the Stokes radiation for generation from spontaneous noises, for the gain increment $\Gamma = 60$ and $T_2 = 1$ ns in the case of a stepwise switching of the pump. It can be seen that the minimum of the intensity coincides in time with the middle of a temporary phase jump.

It should be noted that due to the inertia of the four-wave mixing on the Brillouin nonlinearity the signal in the probe channel is delayed by the time $\sim T_2$ relative to the main Stokes pulse, which in our case is ~ 0.6 ns for CCl_4 and ~ 1.5 ns for $TiCl_4$ (Fig. 9, see also [10]). This fact must be taken into account when determining the exact time delay of the intensity minima of the main Stokes pulse relative to the probe pulse. With all the above considerations taken into account, using the experimentally measured time delays we obtained the following propagation velocities of Brillouin dark solitons in the bulk of the active medium: $V \sim 5 \times 10^7$ m s^{-1} for CCl_4 and $\sim 2 \times 10^7$ m s^{-1} for $TiCl_4$, which, for example for $TiCl_4$, is about 10 times less than the phase velocity of light in this material.

Note also that the experiments performed on the setup (Fig. 2) and the virtual experiment allowed us to answer the question whether the process of attainment of the stationary scattering regime is wave-like as is stated in [13]. It is clearly seen (Figs 4 and 7) that the leading edges of main and probe pulses appear almost simultaneously. This unambiguously indicates a monotonic (along the entire interaction length) increase in the intensity at the leading edge of the Stokes wave and the absence of the process as such.

3. Conclusions

Thus, using the experiments and computer model of the process we have shown that the SBS generation from spontaneous noises has unstable time parameters due to stochastic initial conditions. This can lead to generation of Stokes Brillouin solitons, which is manifested in the appearance of

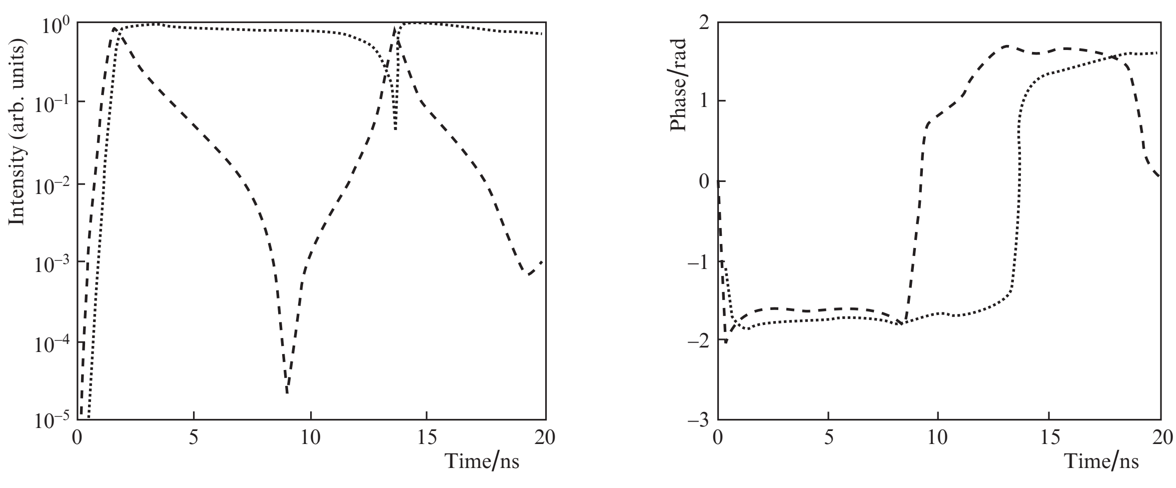

Figure 8. Time dependences of the intensity and phase of the Stokes signal (dotted curves) and the Stokes signal in the probe channel (dashed curves) in the case of stepwise switching of the pump in the regime of generation from spontaneous noises.

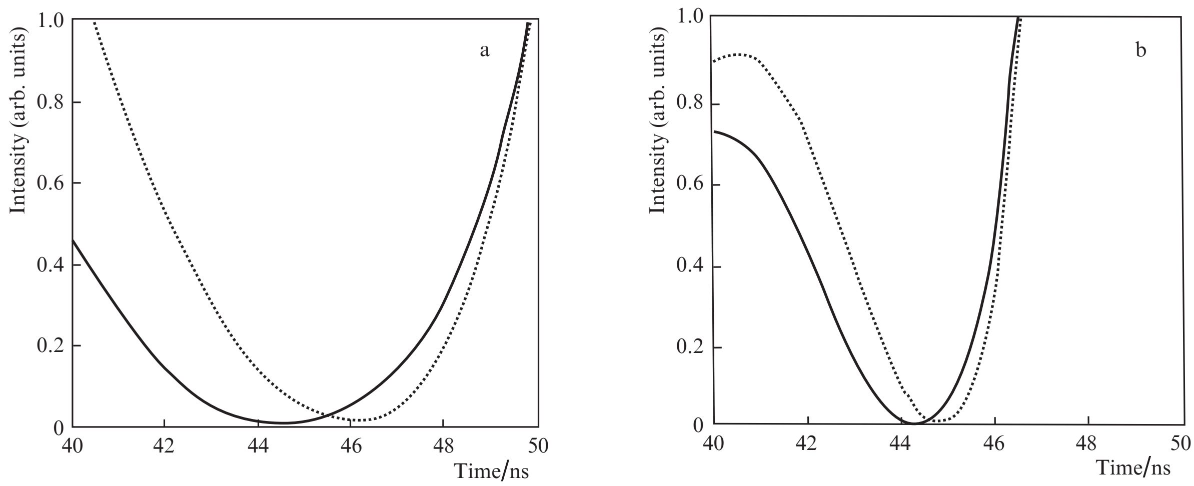

Figure 9. Delay of the pulse reflected in the probe channel (solid curves) with respect to the main Stokes pulse (dashed lines) in the region of generation of dark solitons for $TiCl_4$ (a) and CCl_4 (b).

the jump-like amplitude and phase modulation of the output radiation. The propagation velocity of solitons in a short active medium at a small excess over the threshold is determined by the increment of the stationary threshold gain and the damping time of acoustic waves.

References

1. Anikeev I.Yu., Gordeev A.A., Zubarev I.G., Mironov A.B., Mikhailov S.I. *Kvantovaya Elektron.*, **14**, 207 (1987) [*Sov. J. Quantum Electron.*, **17**, 124 (1987)].
2. Anikeev I.Yu., Gordeev A.A., Zubarev I.G., Mironov A.B., Mikhailov S.I. *Kvantovaya Elektron.*, **17**, 295 (1990) [*Sov. J. Quantum Electron.*, **20**, 235 (1990)].
3. Wiggins T.A., Wick R.W., Rank O.H. *Appl. Opt.*, **5** (6), 1069 (1966).
4. Erokhin A.I., Starunov V.S. *Kr. Soobshch. Fiz. FIAN*, (4), 18 (2000).
5. Metin S.M., Ottusch J.J., Crispin J.D., Rockwell D.A. *Phys. Rev. Lett.*, **68** (11), 1702 (1992).
6. Akhmanov S.A., D'yakov Yu.E., Chirkin A.S. in: *Vvedenie v staticheskuyu radiofiziku i optiku* (Introduction to Statistical Radiophysics and Optics) (Moscow: Nauka, 1981) p. 134.
7. Yasuhiro, Midorikawa, Obara, Tashiro. *J. Opt. Soc. Am. B*, **8** (12), 2459 (1991).
8. Chulkov R.V., Grabtchikov A.S., Lisinetckii V.A., Orlovich V.A., Chehlov O.V. *J. Opt. Soc. Am. B*, **24** (11), 2829 (2007).
9. Gordeev A.A., Efimkov V.F., Zubarev I.G., Mikhailov S.I., Sobolev V.B. *Kvantovaya Elektron.*, **20**, 1005 (1993) [*Quantum Electron.*, **23**, 875 (1993)].
10. Efimkov V.F., Zubarev I.G., Kotov A.V., Mikhailov S.I., Mironov A.B., Pasmanik G.A., Shilov A.A. *Zh. Eksp. Teor. Fiz.*, **77**, 526 (1979).
11. Dianov E.M., Karasik A.Ya., Lutchnikov A.V., Pilipetskii A.N. *Opt. Quantum Electron.*, **21,** 381 (1989).
12. Fotiadi A.A., Kiyan R., Deparis O., Mégret P., Blondel M. *Opt. Lett.*, **27** (2), 83 (2002).
13. Zel'dovich B.Ya., Pilipetskii N.F., Shkunov V.V., in: *Obrashchenie volnovogo fronta* (Phase Conjugation) (Moscow: Nauka, 1985) p. 49.

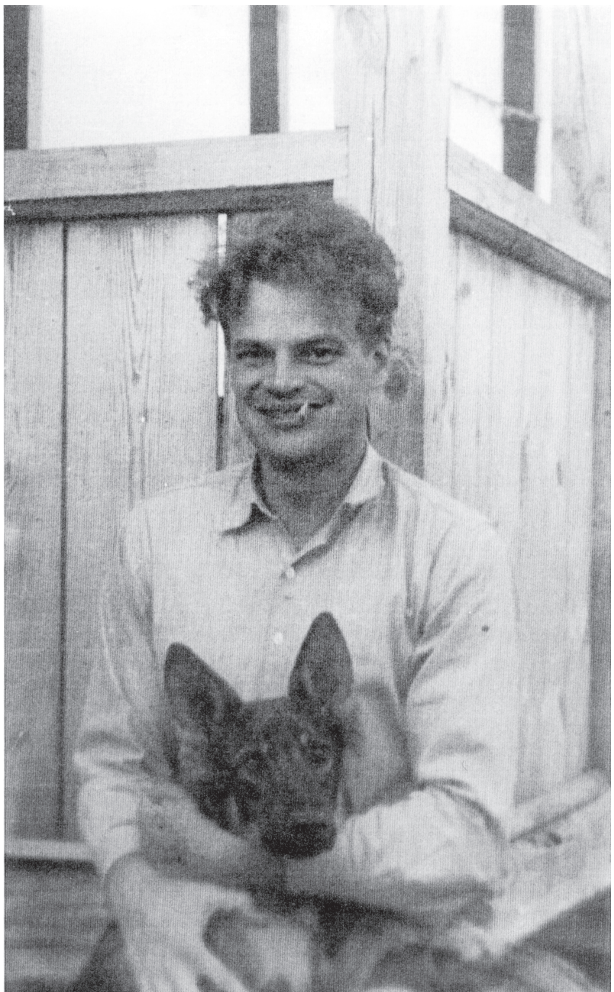

N.G. Basov on vacation at his parents' house in Voronezh (1949).